

Non-destructive functionalization of graphene by surface initiated atom transfer radical polymerization: an ideal nanofiller for poly(p-phenylene benzobisoxazole) fibers

Zhen Hu,^{†,*} Qing Shao,[†] Mark G. Moloney,[‡] Xirong Xu,[†] Dayu Zhang,[†] Jun Li,[†] Chunhua Zhang,[†] Yudong Huang^{†,*1}

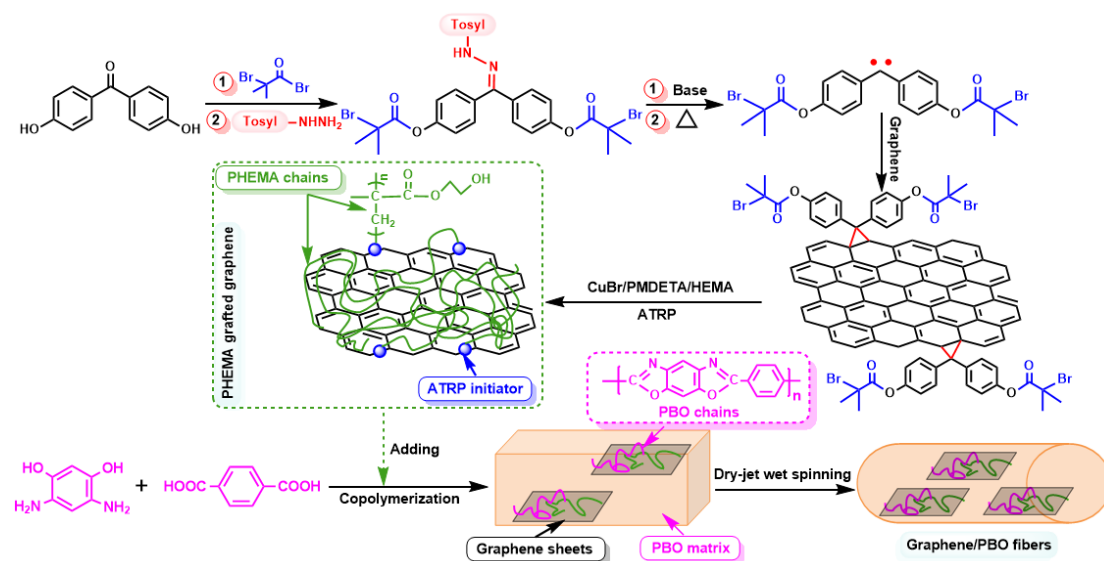
[†] School of Chemistry and Chemical Engineering, MIIT Key Laboratory of Critical Materials Technology for New Energy Conversion and Storage, Harbin Institute of Technology, Harbin 150001, China.

[‡] Department of Chemistry, Chemistry Research Laboratory, University of Oxford, Oxford. OX1 3TA, UK

Abstract: A direct and non-destructive strategy for growing polymers directly from the surface of graphene is demonstrated. The technique involves the covalent attachment of an initiator via one-step cycloaddition of a diarylcarbene, followed by the polymerization of hydroxypropyl methacrylate using atom transfer radical polymerization (ATRP). The functionalization strategy is shown to significantly increase the solubility of the resulting materials (PHEMA-G), and leave the structure of the graphene largely intact. Importantly PHEMA-G/poly(p-phenylene benzobisoxazole) (PBO) composite fibers could be obtained by a one-pot polymerization and dry-jet wet spinning process. The nanocomposite fibers exhibited a tensile strength of 3.22 GPa (51.2% higher than PBO) and Young's modulus of 139.3 GPa (33.7% higher than PBO) at very low PHEMA-G loading (1.0 wt%). This represents an excellent reinforcing efficiency, better than other reports of the graphene/PBO fibers system, and indicates that this material is suitable for applications in composite science,

¹ *Corresponding author. E-mail: yudonghuang@163.com (Yudong Huang), huzhen@hit.edu.cn (Zhen Hu); Fax: +86-451-86413711

For Table of Contents use only



Title: Non-destructive functionalization of graphene by surface initiated atom transfer radical polymerization: an ideal nanofiller for poly(p-phenylene benzobisoxazole) fibers

Author: Zhen Hu*, Qing Shao, Xirong Xu, Dayu Zhang, Jun Li, Yudong Huang*

A facile and non-destructive strategy for growing polymers directly from the surface of graphene is demonstrated. The technique involves the covalent attachment of initiators via one-step cycloaddition of diarylcarbene, followed by the ATRP of various polymers. The obtained modified graphene significantly enhanced the mechanical properties of PBO, which is relatively high value and reinforcing efficiency so far among the reports of the graphene/PBO fibers system.

Introduction

The unique structures and properties of nanomaterials provides fascinating opportunities for material science ¹, and in particular, the combination of nanomaterials and polymers has led to the generation of novel composites with unusual properties ². As the rising star of the carbon family, graphene has already attracted tremendous interest in composite science. Compared to other carbon fillers, such as carbon nanotubes, and carbon nanofibers, its physical properties ³⁻⁶ and cheap fabricating cost ⁷ make graphene the material of choice for the next-generation nanofillers of polymer nanocomposites. However, it is difficult to disperse graphene in suitable solvents due to the high cohesive interaction of graphene sheets. This lack of homogenous dispersion causes fragile interfacial interactions between graphene and a polymer matrix and further limits its utilization in many potential applications ^{8,9}. To overcome the potential effects caused by aggregation, polymer functionalization of graphene is a promising strategy, since it both reduces the cohesive interaction significantly but also increases the interfacial interaction between the graphene and matrix.

For the modification of graphene with polymers by covalent modification, two promising approaches, "grafting to" and "grafting from", have been widely used. Compared to the "grafting to" method, the major advantages of "grafting from" technique is that the higher molecular weight polymer chains can be grafted and a better coverage ratio of polymers on graphene can be achieved. Atom transfer radical polymerization (ATRP) is one of the most widely used "grafting from" methods to prepare polymer-modified graphene¹⁰. In previous work, several monomers have been already polymerized from the surface of graphene via ATRP, such as styrene¹¹⁻¹⁴,

methacrylic acid^{15, 16}, acryl amide¹⁷, methacrylamide¹⁸, t-butyl acrylate^{19, 20}, dimethyl aminoethyl methacrylate²¹, and 2-(ethyl(phenyl)amino)ethyl methacrylate²², among others. Generally, ATRP is associated with the polymerization of monomers from initiators on the graphene, which requires the initial introduction of ATRP initiators. Using the rich chemistry of hydroxyl, carboxyl, and epoxy groups, graphene oxide (GO) is often selected as the starting material for the covalent attachment of ATRP initiators on its surface by amidation or esterification^{10-12, 15-19, 21}. However, it is well-known that the harsh strong oxidising treatments applied to graphene to make GO cause an inevitable rehybridization of some sp² carbon atoms into the sp³ configuration, disrupting the conjugated structure of graphene and affecting its mechanical, electronic and optical properties²³. In order to maintain the integrity of the structure of graphene, it is not surprising that some work on the direct modification of graphene has been achieved using diazonium salts^{13, 14, 22}. However, this approach uses multiple steps to introduce ATRP initiators. Thus, diazonium molecules having hydroxyl groups are attached to the graphene first, and then, the ATRP initiators are attached at the hydroxyl groups via esterification reaction. Although this strategy has been successful, the search for non-destructive and more direct ways of attachment of ATRP initiators is highly desirable.

Poly(p-phenylene benzobisoxazole) (PBO), one of the representative rigid-rod polymers, is characterized by excellent mechanical and thermal properties. To further enhance the properties of PBO, graphene has been considered as effective reinforcing or functional filler. In previous studies, graphene/PBO nanocomposites were prepared via amidation or esterification using GO as starting materials²⁴⁻²⁷. Most recently, novel reduced GO/ polybenzoxazole nanocomposites were prepared via an ATRP method¹⁰. However, challenges still remain, mainly from the difficult

initial dispersion of the graphene in PBO media or complicated preparation methods. The development of a direct, efficient strategy for the preparation of the composites would represent a significant advance. To accomplish this goal, In this paper, we describe an approach in which ATRP initiators were introduced to pristine graphene via a one-step carbene reaction, which can be further polymerized by ATRP to give various graphene/polymer composites. Grafting poly(2-hydroxyethyl methacrylate) (PHEMA) would improve the solubility, dispersity, interfacial adhesion and even reactivity of graphene in PBO matrix. This material could then be readily blended with PBO via in situ polymerization. The hydroxyl groups in HEMA allow for a critical covalent bond formation between the PBO fiber and the nanofiller. Finally, graphene/PBO composite fibers were fabricated using dry-jet wet spinning process. The typical procedure for preparing graphene/PBO composite fibers is presented in Fig. 1.

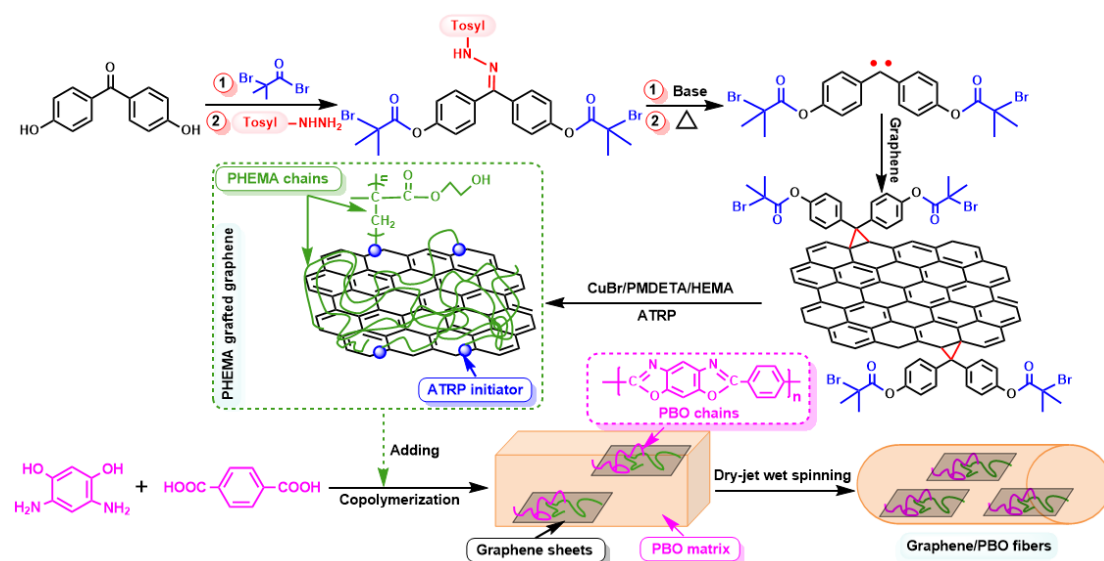


Fig. 1 Non-destructive modification of graphene via surface initiated ATRP and the procedure for composite fibers fabrication

2. Methods and materials

2.1 Materials

The 4, 4'-dihydroxybenzophenone, tosylhydrozone, 2-bromoisobutyryl bromide, triethylamine, N,N,N',N'',N''-pentamethyldiethylenetriamine (PMDETA), 2-hydroxyethyl methacrylate (HEMA), terephthalic acid (TA), polyphosphoric acid (PPA), CuBr, NaNH₂ and common solvent were products of Aladdin, China. The graphene powder was supplied by Hefei Vigon Material Technology Co. Ltd. The monomer for polymerizing PBO, 4, 6-diaminoresorcinol dihydrochloride (DAR•2HCl), was synthesized in our laboratory from 1, 2, 3-trichlorobenzene^{26, 28}.

2.2 The synthesis of tosylhydrazone derivative as carbene precursor

In order to introduce ATRP initiators to carbene precursor, the initiator segments were reacted with 4, 4'-dihydroxybenzophenone via esterification. The 4, 4'-dihydroxybenzophenone (1.07 g, 0.5 mmol) and triethylamine (4.58 mL, 1.65 mmol) were dissolved in 50 mL tetrahydrofuran (THF). 2-Bromoisobutyryl bromide (1.48 mL, 1.2 mmol) was added slowly to the above solution and reacted for 20 h with stirring at room temperature. The product was recrystallized from THF/methanol (30 mL/50 mL) to give a light yellow powder (compound *a*). Yield: 72%. ¹H NMR (CDCl₃, 400 MHz, δ): 2.03, 7.20, 7.82 ppm. ¹³C NMR (CDCl₃, 400 MHz, δ): 30.7, 54.9, 121.2, 131.7, 135.2, 154.0, 169.7, 197.1 ppm. IR: 2980, 1751, 1647, 1597, 1502, 1456, 1158, 928, 885, 759, 676, 658 cm⁻¹. MS m/z (%): 513.0 (75.7), 434.3 (100). The characterization spectra were shown in Fig. S1.

To prevent the side reaction of ATRP initiator segments of compound *a*, the present study used tosylhydrazone to modify the ketone. We found that this mild approach could form N'-(diphenylmethane) benzenesulfonohydrazide derivative (compound *b*), which contained ATRP initiator groups after the reduction. The obtained compound *a* (0.2 mmol) was added to mixing solution of EtOH/THF (volume ratio: 1:1) and tosylhydrazone (0.4 mmol) was added. The

obtained mixture was refluxed at 80 °C for 48 h with stirring. The solvent was removed in vacuum, and the obtained product was purified by column to give compound *b*. Yield: 73.3%. ¹H NMR (CDCl₃, 400 MHz, δ): 2.03, 2.37, 7.00, 7.13, 7.25, 7.51, 7.77 ppm. ¹³C NMR (CDCl₃, 400 MHz, δ): 21.4, 30.5, 55.1, 121.1, 127.9, 129.9, 135.3, 144.1, 152.0, 169.9 ppm. IR: 3210, 2979, 1752, 1600, 1505, 1462, 1263, 1161, 1136, 1101, 880, 815, 666 cm⁻¹. MS m/z (%): 681.0 (100). The characterization spectra were shown in Fig. S2.

2.3 Non-destructive carbene cycloaddition of graphene

The tosylhydrazone derivative (compound *b*) was deprotonated to reveal a diaryldiazo that could be converted into carbene. The compound *b* (0.2 mmol) was dissolved in dry CH₂Cl₂ and NaNH₂ (2 mmol) was added to the above solution to remove the tosyl groups. The mixture was reacted in the dark at room temperature for 6 h to give a dark pink solution (compound *c*). As this diaryldiazo compound *c* was unstable, we could not obtain the correct NMR and MS spectra. However, FT-IR has shown effective evidence that the compound *c* was prepared successfully. IR: 2923, 2022, 1753, 1599, 1504, 1461, 1268, 1161, 1136, 1036, 891, 671 cm⁻¹. The characteristic peaks at 2022 and 671 cm⁻¹ were observed and resulted from the presence of diazo and C-Br groups of compound *c*, respectively.

The pristine graphene was added into the above solution containing compound *c*. The solvent was removed under vacuum to adsorb compound *c* onto the graphene powder. The solid mixture was heated to 120 °C for 30 min to generate diarylcarbene, and react it by covalent bond formation onto the graphene surface. The final product (Init-G) was washed with acetone and water for several times to remove the impurity and adsorbed compounds.

2.4 Surface initiated ATRP of graphene

PHEMA was grafted onto graphene oxide???? from the ATRP initiator groups on the surface of Init-G. In a typical polymerization, the Init-G (100 mg, $[I]_G=5.04\times 10^{-5}$ mol) and CuBr powder (7.2 mg, 5.04×10^{-5} mol) were introduced into the flask under a nitrogen flow. PMDETA (17.6 mg, 10.1×10^{-5} mol), HEMA (6.56 g, 5.04×10^{-2} mol) were then added into the flask under N_2 atmosphere. The obtained mixture was stirred at 110 °C for 24 h. The polymerization was stopped by cooling and opening the flask to expose the catalyst to air. The mixture was diluted and washed with THF and filtered with a Teflon filter. The polymer grafted graphene (PHEMA-G) was obtained after drying at 40 °C for 24 h under vacuum (yield 25 mg, 121% on the basis of the Init-G).

2.5 One-pot in situ polymerization of PBO with PHEMA-G

PHEMA-G (0~1.5 wt%, based on the PBO polymer) and 21.60 g of H_3PO_4 (85 wt% in H_2O) were placed in a three-neck round-bottom glass flask, equipped with a mechanical stirrer and a nitrogen inlet/outlet. After sonication for 2 h, 27.05 g P_2O_5 was added in three portions, then TA (8.30 g) was added. An esterification was then carried out at 120 °C for 6 h, in which PHEMA-G was further modified by TA. $DAR\bullet 2HCl$ (10.65 g) was added into the above mixture, and the solution was stirred at 100 °C for 8 h to induce dehydrochlorination. Another 19.50 g of P_2O_5 was then added to the mixture to combine H_2O formed by the polycondensation reaction and bring the P_2O_5 concentration to 83.5 wt%. The resulting polymer solution was heated to 200 °C at 5-10 °C/h stepwise, and kept at 200 °C for 2 h with constant stirring.

2.6 Fabrication of graphene/PBO nanocomposite fibers

A lab-scale spinning system was used for the dry-jet wet-spinning of graphene/PBO nanocomposite fibers. The synthesized polymer solution was transferred to a reactor and heated

at 160 °C for 10 h before spinning under the protection of N₂. The key spinning conditions were as follows: orifice diameter, 0.4 mm; air gap, 300 mm; draw ratio, 10; spinning temperature, 160 °C; and the solvent for coagulation and washing was phosphoric acid and water at room temperature. Fibers wrapped on spools were washed in running water for one day and subsequently dried overnight under vacuum at 80 °C.

2.7 Characterization and measurement

The chemical structure of organic compounds was investigated by FT-IR, NMR and MS analysis. Infrared (IR) spectra were recorded on Bruker Tensor 27 FT-IR spectrometers. ¹H NMR and ¹³C NMR were recorded on Bruker AVF400 (400 MHz) spectrometer. Mass spectra (m/z) were obtained with a Fisons Platform spectrometer with electrospray ionisation (ESI). The modified graphene was characterized by FT-IR, Raman, XPS, TGA, TEM and AFM. Raman spectra were detected using a LabRam-1B Raman micro spectrometer at 632.8 nm (Horiba Jobin Yvon, France). XPS was performed on lab-built spectrometers at 10⁻⁹ - 10⁻¹⁰ Torr, with an Al K-α X-ray source (1486.6 eV). TG analyses were performed with a thermogravimetric analyzer (Netzsch STA449C) from room temperature to 850 °C in air at a heating rate of 10 °C min⁻¹. TEM (JEOL, JEM-2100F) and AFM (Sounding Housing SPA 400) were used to characterize the morphology and structure of the graphene samples. For tensile testing, composite fibers were mounted on cardboard tabs. Testing was performed on a universal tensile tester (model WD-1) using 2.00 cm gage length at a strain rate of 2%/min. The fiber diameter was measured with an optical microscope (equipped with CCD, CAMERAL). Fifty samples were tested in each case.

3. Results and discussion

3.1 The non-destructive modification of graphene via surface initiated ATRP

The preparation of polymer-functionalized graphene often needs harsh chemical attacks, which seriously damages the properties of graphene ²⁹⁻³¹. Against the above background, we developed a novel and mild approach to prepare diarylcarbene with ATRP initiator groups, aiming to generate a graphene surface decorated with desired polymer chains. The diarylcarbene derivatives permitted a controlled introduction of ATRP initiator segments to graphene via a one-step reaction, which forms the basis for the subsequent polymer modification. By controlling the monomer, a variety of graphene polymer hybrids can be obtained by ATRP, ranging from simple linear polymer to sophisticated star brush copolymers. The present study uses HEMA as monomer to introduce PHEMA onto the graphene surface. The PHEMA contains abundant hydroxyl groups, which may participate in the subsequent polycondensation of PBO ²⁸. The dispersability of PHEMA-G was examined in water, ethanol, DMF, THF, and acetone. The PHEMA-G is well dispersed in water, ethanol and DMF due to good interaction between hydroxyl groups of PHEMA and polar solvents, but relatively badly dispersed in acetone (Fig. S4).

The non-destructive functionalization of the graphene was confirmed by FT-IR spectroscopy, and the results are shown in Fig. 2a. The pristine graphene shows strong bands at $\sim 1640\text{ cm}^{-1}$ and $\sim 2940\text{ cm}^{-1}$ corresponding to the C=C and C-H stretching of the graphene structure. After diarylcarbene addition, characteristic peaks at ~ 1740 and $\sim 1280\text{ cm}^{-1}$ in the Init-G spectrum related to the new ester bond were easily detected. A characteristic bond is also seen at 670 cm^{-1} corresponding to C-Br bond. These FTI-R results provide direct evidence for covalent bonding between graphene and diarylcarbene with ATRP initiator. After ATRP of HEMA, the characteristic peak at $\sim 3450\text{ cm}^{-1}$ related to the OH groups becomes broader and stronger due to the existence

of hydroxyl groups in the structure of PHEMA. Does the C-Br bond resonance disappear? The stretching vibration of carbonyl groups of HEMA at $\sim 1740\text{ cm}^{-1}$ proves that PHEMA is attached onto the Init-G surface. However, as expected, after PHEMA grafting, the characteristic peaks (such as $\sim 670\text{ cm}^{-1}$) of diarylcarbene are weaker in the PHEMA-G due to the shielding effect of PHEMA chains.

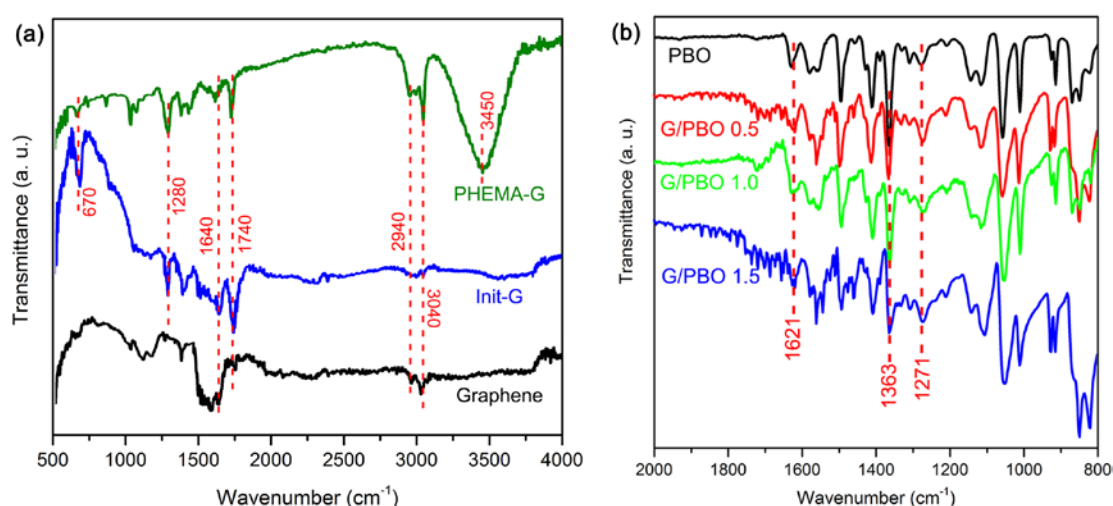


Fig. 2 (a) FT-IR spectra of pristine graphene, Init-G and PHEMA-G, (b) FT-IR spectra of PBO and G/PBO composite fibers.

The covalent link between graphene and PHEMA chains was further confirmed by Raman spectra (Fig. S5). In all samples, two prominent peaks are clearly visible, corresponding to the D, G and 2D bands at ~ 1340 and $\sim 1550\text{ cm}^{-1}$, respectively. The intensity ratio between the D-mode and G-mode (I_D/I_G) is calculated to be 0.82 in the graphene sample. In the Init-G sample, the G band became blue shifted to a slightly higher value of 1573 cm^{-1} while I_D/I_G value was slightly increased (I_D/I_G increased from 0.82 to 1.01). These characteristic changes of Raman spectrum are the result of an increasing amount of sp^3 bonds formation, which could be strong evidence of chemical functionalization³². There is no significant change in I_D/I_G values of PHEMA-G ($I_D/I_G=1.02$). This indicates that the subsequent ATRP processes did not change the structure of

the Init-G sample.

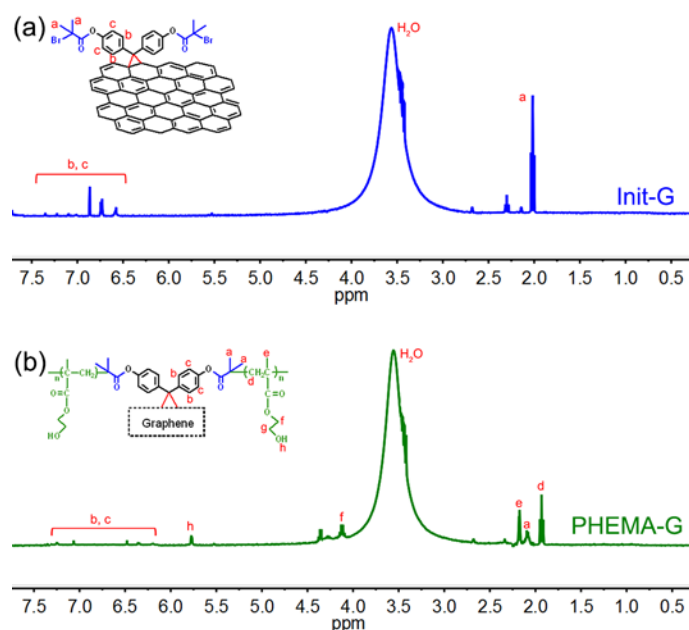


Fig. 3 Solid state ^1H NMR spectra of (a) Init-G and (b) PHEMA-G.

NMR has been a useful tool to provide valuable information on covalently functionalized graphene. Fig. 3 shows the ^1H NMR spectra for the Init-G and PHEMA-G samples. After the cycloaddition of diarylcarbene (Fig. 3a), Init-G shows aromatic ring signals at 6.50-7.50 ppm which are consistent with the attachment of diarylcarbene. Furthermore, the signal at 2.01 ppm may be attributed to the $-\text{CH}_3$ of ATRP initiator segment. After ATRP of HEMA (Fig. 3b), the characteristic signals of PHEMA chains for PHEMA-G are as follows: $\delta(\text{C}(\text{CH}_2), \text{d})=1.92$ ppm, $\delta(\text{C}(\text{CH}_3), \text{e})=2.17$ ppm, $\delta(\text{COO}(\text{CH}_2), \text{f})=4.11$ ppm, $\delta(\text{OH}, \text{h})=5.76$ ppm³³. The ^1H NMR spectrum of the PHEMA-G also shows resonances from benzene rings at 6.50-7.50ppm and isobutyl bromide CH_2 signal at 2.07 ppm. The broad signal at ~ 3.54 ppm is related to the absorbed H_2O during the sample preparation and testing. The ^1H NMR results indicate that an efficient polymer functionalization of the graphene has been achieved via novel surface initiated ATRP. Moreover, the length of grafted PHEMA chains on graphene could be analyzed by ^1H NMR spectroscopy.

Using end-group analysis (integral area ratio of peaks a to e), the degree of polymerization ($DP \approx 10.8$) and number average molecular weight ($M_n \approx 1404$) can be calculated for grafted PHEMA chains. Due to the steric hindrance effect of Init-G, it is impossible for all initiators to be involved in the subsequent ATRP of HEMA. That is, the actual M_n of grafted PHEMA chains may higher than the end-group analysis value. On the other hand, this relatively low M_n suggests that surface modification with the diarylcarbene seems to be rather efficient with the various ATRP initiators competing for the available monomer.

TGA was performed on the surface functionalized graphene to study the degree of functionalization as shown in Fig. S6. According to the results, graphene shows excellent thermal stability, and does not show obvious mass loss until ~ 485 °C. For Init-G, a relatively large loss in mass was observed ~ 183 °C which is believed to result from the degradation of diaryl initiator groups on the graphene. At 485 °C, the remaining weight for Init-G is 84.9%, while there is no obvious weight loss for graphene. Assuming that the different weight loss is due to the removal of the grafted diaryl initiator groups, the mole ratio of the ATRP initiator ($[I]_G = 5.04 \times 10^{-4}$ mol/g Init-G) on graphene surface was calculated by using the weight loss (12.5%) and the diaryl initiator molecular weight (496 g/mol). Assuming that all the carbon atoms from the graphene remained at 485 °C, then the mole ratio of carbon can be determined as $0.849/12 = 0.070$ mol/g Init-G. Based on the mole ratio of ATRP initiator and carbon, the grafting density of initiator groups on graphene is estimated to be around 1 in every 139 carbon atoms. After polymerization of HEMA, the PHEMA-G sample showed a significant mass loss at ~ 252 °C which could be related to the decomposition of PHEMA chains grafted onto surface. The content of ATRP initiator and grafted PHEMA could be calculated as 10.0% and 17.0%, respectively ^{34, 35}. Assuming that every

ATRP initiator initiates the polymerization of HEMA, the M_n and DP of grafted PHEMA ($M_n \approx 843$, $DP \approx 6.50$) can be calculated by using the weight loss of PHEMA (17.0%) and mole ratio of the ATRP initiator ($[I]_0 = 4.03 \times 10^{-4}$ mol/g PHEMA-G). This M_n is lower than the value estimated by 1H NMR spectroscopy, which may result from the relatively high carbon residue rate of PHEMA.

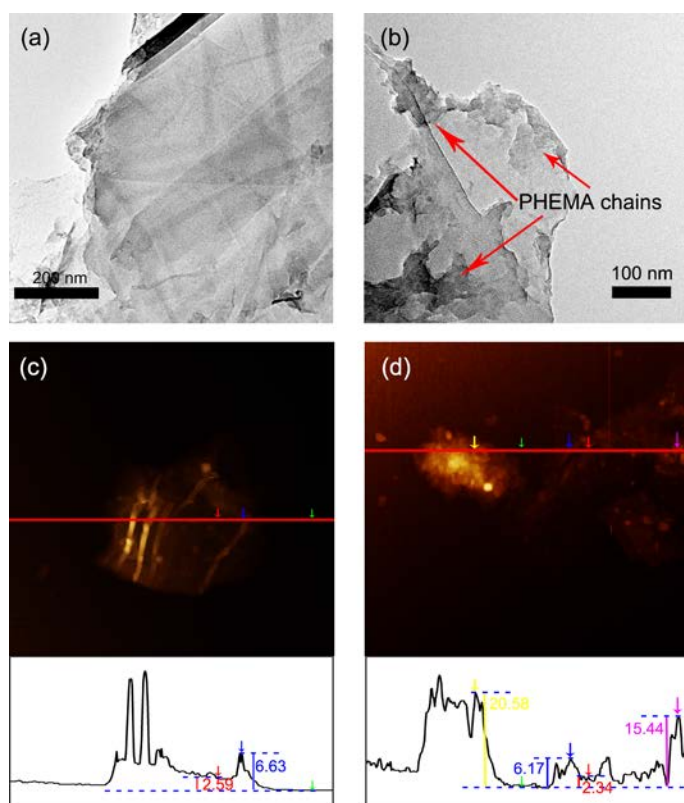


Fig. 4 Representative (a) TEM image of Init-G, (b) TEM image of PHEMA-G, (c) AFM image of Init-G with height profile diagram, (d) AFM image of PHEMA-G with height profile diagram.

To investigate the morphology of modified graphene samples, TEM and AFM were also been performed. As shown in Fig. 4a, the Init-G displays flake-like shapes with wrinkles and pleats. The average height of Init-G sheets is no less than 2.59 nm (Fig. 4c), which is thicker than the well-known van der Waals thickness of pristine graphene sheets (0.34 nm), consistent with the presence of diarylcarbene structure. After polymer functionalization, PHEMA-G is well coated with polymer (Fig. 4b), and the amorphous PHEMA chains form “dark clouds” on the graphene.

Moreover, the PHEMA-G has greater polymer density at its edges, which may be explained by the fact that the amorphous edge carbon atoms are more easily attacked and modified. The thickness of the PHEMA-G is more than 6.0 nm (Fig. 4d), which is much higher than that of graphene or Init-G. This increased thickness further proves the presence of polymeric chains across the graphene surface, which may be caused by their swollen appearance and rough surface³⁶.

3.2 The fabrication of graphene/PBO fibers via on-pot procedure

Despite the great potential as nanofillers, the homogenous dispersal of graphene in polymeric matrices is difficult (especially in the high viscosity PBO solution). Furthermore, the lack of interfacial bonding between graphene and the matrix leads to fiber pullout during stress, followed by catastrophic failure. In the present study, the PHEMA-G was first dispersed in H_3PO_4 solution with relatively low viscosity. Then, PHEMA-G was further modified by TA via esterification using PPA as dehydrating agent. This functionalization not only further increases the solubility and dispersity of PHEMA-G, but also provides covalent bonds with PBO matrix. As the modifier TA is one monomer of PBO, the graphene functionalization and copolymerization can be carried out in one reaction system by a facile, one-pot procedure. The hypothetical reaction mechanism is shown in Fig. 5.

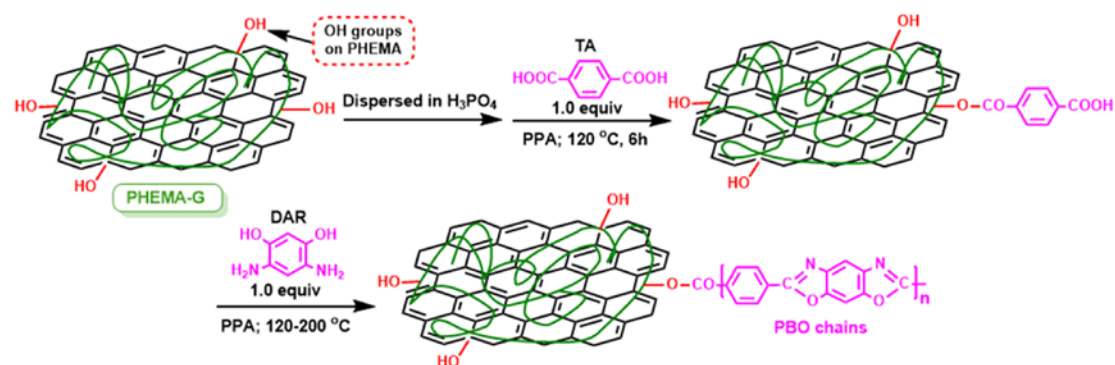


Fig. 5 The possible mechanism of one-pot synthesis of graphene/PBO composites.

Graphene/PBO composites with PHEMA-G compositions of 0.5, 1.0 and 1.5 wt% are recorded as G/PBO 0.5, G/PBO 1.0 and G/PBO 1.5, respectively. The IR spectra of G/PBO were highly similar to PBO, and the results are shown in Fig. 2b. In all the spectra, the peaks at 1621, 1363, and 1271 cm^{-1} were assigned to C=N, C-N, and C_{Ar}-O-C stretches, respectively, indicating the existence of oxazole rings in the polymer³⁷. It would appear that the chemical structure of PBO largely remains intact after the in situ polymerization with graphene.

The morphology of G/PBO fibers was investigated by SEM, shown as Fig. 6. It can be found from the images that the diameter of the fibers is in the range 25~30 μm , and there are few cracks and microfibrils on the fiber surfaces. The outer surface of the G/PBO fibers (especially at 0.5 and 1.0 wt% loading of PHEMA-G) is smoother than PBO fiber. As the surface texture reflects the uniformity of the micro fibrils and polymer chains, the PHEMA-G may prevent polymer chains from fluctuation and rearrangement when coagulated in phosphoric acid and water. That is, the incorporation of PHEMA-G sheets enhances the interaction of micro fibrils and restricts the slippage of the orientated chains, which result in better orientation of PBO chains (further proved by XRD analysis).

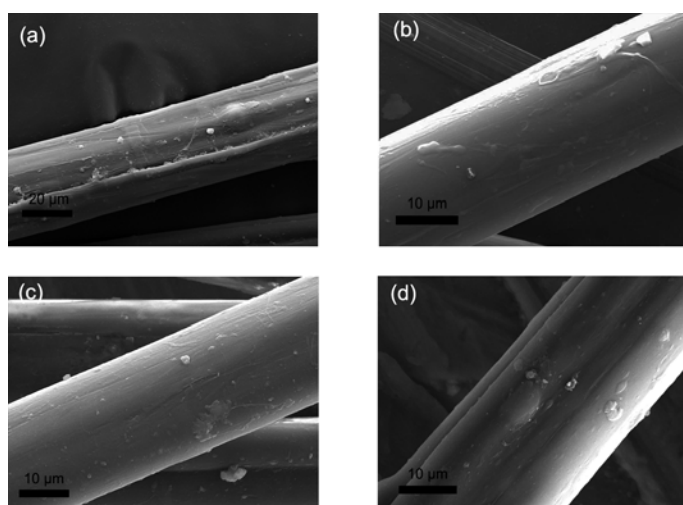


Fig. 6 Representative SEM images of (a) PBO, (b) G/PBO 0.5, (c) G/PBO 1.0, (d) G/PBO 1.5

composite fibers.

PBO is typical lyotropic liquid crystalline polymer; the orientation structure has a great influence on its mechanical properties. It is reported that the carbon nanomaterials (including carbon nanotubes and graphene) are helpful for the packing of PBO molecular chains^{24, 27, 38}. Thus, WAXD patterns along the equatorial directions are used to quantitatively analyze the crystal size of G/PBO fibers (Fig. S7). The WAXD patterns of all samples show two typical diffraction peaks at $\sim 16.0^\circ$ and $\sim 26.7^\circ$, corresponding to the (200) and (010) crystalline plane, respectively. As the content is low, the characteristic peak of graphene at 10.8° is not observed in the patterns of the G/PBO composites. The apparent crystal size (L_{hkl}) of PBO could be computed using Scherrer's equation $L_{hkl} = K\lambda/B\cos\theta_{hkl}$. The results show that G/PBO fibers show higher crystal sizes of 2.76, 4.40 and 4.12 nm for G/PBO 0.5, G/PBO 1.0 and G/PBO 1.5, respectively, compared to 2.20 nm for PBO fibers. As the discussion of our previous work²⁶, this promoting effect of orientation is mainly related to the π - π interaction, covalent interaction and template effect of graphene. We should also note that the crystal size slightly decreases at 1.5 wt% loading of PHEMA-G, which indicates that the relatively high concentration of graphene may hinder the orientation of PBO molecular chains²⁷.

To evaluate the enhancement effect of the PHEMA-G on the mechanical properties of PBO, several G/PBO composite fibers containing different contents of PHEMA-G were prepared and tested (Fig. 7a). Generally, the tensile strength of G/PBO fibers is found to increase with graphene loading in the matrix. As nanofiller, the pristine graphene also presented an obvious enhancement effect on the tensile strength of composite fibers at low loading. However, the PHEMA-G exhibits more a pronounced increasing strength than graphene. For instance, the

strength of the composite fiber is greatly enhanced by 51.2% (from 2.13 to 3.22 GPa) at 1.0 wt% loading of PHEMA-G. Compared to the previous studies, 1.0 wt% modified carbon nanotubes²⁸ and graphene²⁷ exhibited increases of 34.5% and 11.9% in tensile strength of PBO, respectively. This better improvement of PHEMA-G in the tensile strength may be attributed to the better dispersion in the matrix, the covalent links between the PHEMA-G and PBO chains, and the non-destructive modification strategy of graphene. The Young's modulus data for the G/PBO fibers shows a similar increase as the tensile strength (Fig. 7b). For the composite fiber with 1.0 wt% of PHEMA-G, the modulus increases from 104 to 139 GPa, corresponding to 33.7% increase. This enhancement is very significant with such a relatively low PHEMA-G content. It is worth noting that further increasing the PHEMA-G loading at 1.5 wt% led to a slowdown in the increase rate of both tensile strength and modulus. It is assumed that the relatively high PHEMA-G loading might restack and lead to agglomeration, saturating the reinforcing efficiency. On the other hand, crystallization behavior would affect the strength and modulus of the PBO fibers. The decreased orientation degree and crystal size might also account for the slowdown in the increase rate. In order to further estimate the PHEMA-G dispersion and alignment in the PBO fibers, a rule-of-mixtures calculation was performed using the Halpin-Tsai equations, which assumes the graphene orientation dispersed in the PBO matrix^{26,27}. The Young's modulus of the graphene and PBO is 1 TPa and 104 GPa, respectively. The thickness and average length of graphene are set as 2.5 nm and 1 μm according to the AFM and TEM results. The density of the graphene is 1.60 and the PBO is 1.56 g/cm³. It can be seen from Fig. 7b that the tensile modulus of G/PBO fibers is obviously higher than the theoretical predictions for the copolymer in which graphene are aligned along the fiber axis. The results indicate that PHEMA-G is highly aligned in the PBO matrix

formed via the dry-jet wet spinning process.

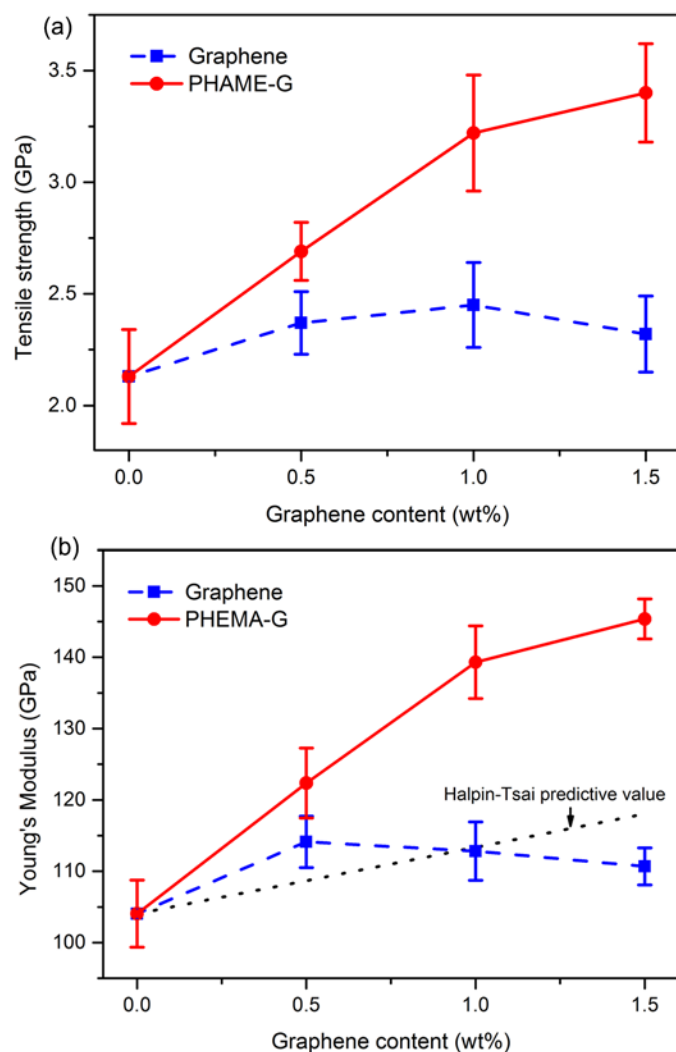


Fig. 7 (a) Tensile strength changes of PBO composite fibers with increasing graphene content. (b) Young's modulus of G/PBO composite fibers and the theoretical results from the Halpin-Tsai equation.

The thermal behaviors of G/PBO composite fibers were studied by TG in air (Fig. S8). PBO fibers start to degrade at around 500 °C, which is associated with the catastrophic decomposition of PBO chains. The onset decomposition temperatures ($T_{10\%}$) of PBO, G/PBO 0.5, and G/PBO 1.0 are 482.8, 522.4, and 539.7, respectively, which indicates that the composite fibers maintain better heat resistance than PBO. Furthermore, the residual carbon contents of G/PBO 1.5 fibers (31.7%)

are much higher than PBO fiber (13.2%) at 800 °C. The inherent viscosity is further measured in MSA solution by an Ubbelohde viscometer. The viscosity of PBO, G/PBO 0.5, G/PBO 1.0, and G/PBO 1.5 is 21.9, 20.7, 25.6 and 28.3 dL/g, respectively. Considering that we have used the same polymerization conditions, the difference of molecular weight should not be so significant between PBO and G/PBO composites. The difference of the viscosity is more likely to be the result of the generation of crosslinking structures. In the present study, the PHEMA-G has multiple epoxy groups, which can react with the PBO chains and serve as cross linkers. The three-dimensional crosslinked structure will further enhance the char formation degree of PBO. It can be concluded that incorporation of PHEMA-G improves the thermal stability of PBO matrix and the flame retardancy of PBO. Consequently, we believe this novel and efficient method is helpful for constructing desired graphene/polymer nanocomposites, which would further develop high-performance graphene-based materials.

Conclusions

In summary, we have demonstrated a facile and non-destructive method to directly functionalize graphene using ATRP. The modification was performed by attaching the initiator to pristine graphene by one-step cycloaddition of diarylcarbene, followed by the ATRP of HEMA through the “grafting-from” strategy. The resulting PHEMA-G was characterized by FT-IR, Raman, ¹H NMR, TGA, AFM, and TEM analysis, and the nanocomposites showed excellent dispersability in common organic solvents and water. This increased dispersability and intact structure enhanced the potential of PHEMA-G for applications in polymer composites. PHEMA-G was readily blended with PBO via one-pot polymerization to fabricate PHEMA-G /PBO composite fibers. The FT-IR,

SEM, and XRD analyses of the composite fibers indicated that PBO retained structural features seen in virgin samples while PHEMA-G showed obvious promoting effect of PBO orientation. Mechanical property measurements revealed that the PMEHA-G/PBO fibers exhibited a tensile strength (3.22 GPa) and Young's modulus (139.3 GPa) at very low PMEHA-G loading 1.0 wt%, corresponding to 51.2% and 33.7% increase compared to the PBO fibers, respectively. Meanwhile, TG was used to study the influence of PMEHA-G on the thermal stability of PBO. It was found that the initial thermal degradable temperature (T5%) of PBO was improved by 97 °C after introduction of 1 wt % PMEHA-G. The increased dispersability, compatible interfacial interaction between PHEMA-G and PBO, and non-destructive modification strategy of graphene has been suggested as the main reasons for the performance improvement of PBO.

Acknowledgements

We thank the National Natural Science Foundation of China (no. 51673053, 51273050), Key Technologies R & D Program of Heilongjiang Province (no. GA14A101), and the Fundamental Research Funds for the Central Universities (no. HIT. IBRSEM. 2013016).

References:

1. Singh, V.; Joung, D.; Zhai, L.; Das, S.; Khondaker, S. I.; Seal, S., Graphene Based Materials: Past, Present and Future. *Prog. Mater. Sci.* **2011**, *56*, 1178-1271.
2. Balazs, A. C.; Emrick, T.; Russell, T. P., Nanoparticle Polymer Composites: Where Two Small Worlds Meet. *Science* **2006**, *314*, 1107-1110.
3. Chen, C.; Yang, Q.-H.; Yang, Y.; Lv, W.; Wen, Y.; Hou, P.-X.; Wang, M.; Cheng, H.-M., Self-Assembled Free-Standing Graphite Oxide Membrane. *Adv. Mater.* **2009**, *21*, 3007-3011.
4. Li, Y.; Hu, Y.; Zhao, Y.; Shi, G.; Deng, L.; Hou, Y.; Qu, L., An Electrochemical Avenue to Green-Luminescent Graphene Quantum Dots as Potential Electron-Acceptors for Photovoltaics. *Adv. Mater.* **2011**, *23*, 776-780.
5. Avouris, P., Graphene: Electronic and Photonic Properties and Devices. *Nano Lett.* **2010**, *10*,

4285-4294.

6. Balandin, A. A.; Ghosh, S.; Bao, W.; I. Calizo; Teweldebrhan, D.; Miao, F.; Lau, C. N., Superior Thermal Conductivity of Single-Layer Graphene. *Nano Lett.* **2008**, *8*, 902-907.
7. Haddon, R. C., Graphene - the Mother of Two-Dimensional (2-D) Materials. *Acc. Chem. Res.* **2013**, *46*, 2191-2192.
8. Cheng, H. K.; Sahoo, N. G.; Tan, Y. P.; Pan, Y.; Bao, H.; Li, L.; Chan, S. H.; Zhao, J., Poly(Vinyl Alcohol) Nanocomposites Filled with Poly(Vinyl Alcohol)-Grafted Graphene Oxide. *ACS Appl. Mater. Inter.* **2012**, *4*, 2387-2394.
9. Qian, Y.; Lan, Y.; Xu, J.; Ye, F.; Dai, S., Fabrication of Polyimide-Based Nanocomposites Containing Functionalized Graphene Oxide Nanosheets by in-Situ Polymerization and Their Properties. *Appl. Surf. Sci.* **2014**, *314*, 991-999.
10. Chen, Y.; Zhang, S.; Liu, X.; Pei, Q.; Qian, J.; Zhuang, Q.; Han, Z., Preparation of Solution-Processable Reduced Graphene Oxide/Polybenzoxazole Nanocomposites with Improved Dielectric Properties. *Macromolecules* **2015**, *48*, 365-372.
11. Fang, Z.; Ito, A.; Stuart, A. C.; Luo, H.; Chen, Z.; Vinodgopal, K.; You, W.; Meyer, T. J.; Taylor, D. K., Soluble Reduced Graphene Oxide Sheets Grafted with Polypyridylruthenium-Derivatized Polystyrene Brushes as Light Harvesting Antenna for Photovoltaic Applications. *ACS Nano* **2013**, *7*, 7992-8002.
12. Roghani-Mamaqani, H.; Haddadi-Asl, V.; Khezri, K.; Salami-Kalajahi, M., Polystyrene-Grafted Graphene Nanoplatelets with Various Graft Densities by Atom Transfer Radical Polymerization from the Edge Carboxyl Groups. *RSC Adv.* **2014**, *4*, 24439-24452.
13. Fang, M.; Wang, K.; Lu, H.; Yang, Y.; Nutt, S., Covalent Polymer Functionalization of Graphene Nanosheets and Mechanical Properties of Composites. *J. Mater. Chem.* **2009**, *19*, 7098-7105.
14. Fang, M.; Wang, K.; Lu, H.; Yang, Y.; Nutt, S., Single-Layer Graphene Nanosheets with Controlled Grafting of Polymer Chains. *J. Mater. Chem.* **2010**, *20*, 1982-1992.
15. Layek, R. K.; Samanta, S.; Chatterjee, D. P.; Nandi, A. K., Physical and Mechanical Properties of Poly(Methyl Methacrylate) -Functionalized Graphene/Poly(Vinylidene Fluoride) Nanocomposites: Piezoelectric β Polymorph Formation. *Polymer* **2010**, *51*, 5846-5856.
16. Gonçalves, G.; Marques, P. A. A. P.; Barros-Timmons, A.; Bdkin, I.; Singh, M. K.; Emami, N.; Grácio, J., Graphene Oxide Modified with PMMA via ATRP as a Reinforcement Filler. *J. Mater. Chem.* **2010**, *20*, 9927-9934.
17. Ren, L.; Huang, S.; Zhang, C.; Wang, R.; Tjiu, W. W.; Liu, T., Functionalization of Graphene and Grafting of Temperature-Responsive Surfaces from Graphene by ATRP "on Water". *J. Nanopart. Res.* **2012**, *14*, 940-948.
18. Chang, L.; Wu, S.; Chen, S.; Li, X., Preparation of Graphene Oxide-Molecularly Imprinted Polymer Composites Via Atom Transfer Radical Polymerization. *J. Mater. Sci.* **2010**, *46*, 2024-2029.
19. Lee, S. H.; Dreyer, D. R.; An, J.; Velamakanni, A.; Piner, R. D.; Park, S.; Zhu, Y.; Kim, S. O.; Bielawski, C. W.; Ruoff, R. S., Polymer Brushes Via Controlled, Surface-Initiated Atom Transfer Radical Polymerization (ATRP) from Graphene Oxide. *Macromol. Rapid Commun.* **2010**, *31*, 281-288.
20. Li, G. L.; Liu, G.; Li, M.; Wan, D.; Neoh, K. G.; Kang, E. T., Organo- and Water Dispersible Graphene Oxide-Polymer Nanosheets for Organic Electronic Memory and Gold Nanocomposites. *J. Phys. Chem. C* **2010**, *114*, 12742-12748.
21. Yang, Y.; Wang, J.; Zhang, J.; Liu, J.; Yang, X.; Zhao, H., Exfoliated Graphite Oxide Decorated by Pdmaema Chains and Polymer Particles. *Langmuir* **2009**, *25*, 11808-11814.
22. Wang, D.; Ye, G.; Wang, X.; Wang, X., Graphene Functionalized with Azo Polymer Brushes:

Surface-Initiated Polymerization and Photoresponsive Properties. *Adv. Mater.* **2011**, *23*, 1122-1125.

23. Liu, J.; Tang, J.; Gooding, J. J., Strategies for Chemical Modification of Graphene and Applications of Chemically Modified Graphene. *J. Mater. Chem.* **2012**, *22*, 12435-12452.

24. Chen, Y.; Zhuang, Q.; Liu, X.; Liu, J.; Lin, S.; Han, Z., Preparation of Thermostable PBO/Graphene Nanocomposites with High Dielectric Constant. *Nanotechnology* **2013**, *24*, 245702-245712.

25. Choudhury, A., Preparation and Characterization of Nanocomposites of Poly-P-Phenylene Benzobisthiazole with Graphene Nanosheets. *RSC Adv.* **2014**, *4*, 8856-8866.

26. Hu, Z.; Li, N.; Li, J.; Zhang, C.; Song, Y.; Li, X.; Wu, G.; Xie, F.; Huang, Y., Facile Preparation of Poly(P-Phenylene Benzobisoxazole)/Graphene composite Films Via One-Pot in Situ Polymerization. *Polymer* **2015**, *71*, 8-14.

27. Li, Y.; Li, J.; Song, Y.; Hu, Z.; Zhao, F.; Huang, Y., In Situ polymerization and Characterization of Graphene Oxide-co-Poly(Phenylene Benzobisoxazole) Copolymer Fibers Derived from Composite Inner Salts. *J. Polym. Sci. Pol. Chem.* **2013**, *51*, 1831-1842.

28. Hu, Z.; Li, J.; Tang, P.; Li, D.; Song, Y.; Li, Y.; Zhao, L.; Li, C.; Huang, Y., One-Pot Preparation and Continuous Spinning of Carbon Nanotube/Poly(P-Phenylene Benzobisoxazole) Copolymer Fibers. *J. Mater. Chem.* **2012**, *22*, 19863-19871.

29. Young, R. J.; Kinloch, I. A.; Gong, L.; Novoselov, K. S., The Mechanics of Graphene Nanocomposites: A Review. *Compos. Sci. Technol.* **2012**, *72*, 1459-1476.

30. Li, J.; Cui, J.; Yang, J.; Li, Y.; Qiu, H.; Yang, J., Reinforcement of Graphene and Its Derivatives on the Anticorrosive Properties of Waterborne Polyurethane Coatings. *Compos. Sci. Technol.* **2016**, *129*, 30-37.

31. Pathak, A. K.; Borah, M.; Gupta, A.; Yokozeki, T.; Dhakate, S. R., Improved Mechanical Properties of Carbon Fiber/Graphene Oxide-Epoxy Hybrid Composites. *Compos. Sci. Technol.* **2016**, *135*, 28-38.

32. Cancado, L. G.; Jorio, A.; Ferreira, E. H.; Stavale, F.; Achete, C. A.; Capaz, R. B.; Moutinho, M. V.; Lombardo, A.; Kulmala, T. S.; Ferrari, A. C., Quantifying Defects in Graphene Via Raman Spectroscopy at Different Excitation Energies. *Nano Lett.* **2011**, *11*, 3190-3196.

33. Xu, X.; Huang, J., Synthesis and Characterization of Well-Defined Poly(2-Hydroxyethyl Methacrylate-Co-Styrene)-Graft-Poly(ϵ -Caprolactone) by Sequential Controlled Polymerization. *J. Polym. Sci. Pol. Chem.* **2004**, *42*, 5523-5529.

34. Cai, N.; Hou, D.; Luo, X.; Han, C.; Fu, J.; Zeng, H.; Yu, F., Enhancing Mechanical Properties of Polyelectrolyte Complex Nanofibers with Graphene Oxide Nanofillers Pretreated by Polycation. *Compos. Sci. Technol.* **2016**, *135*, 128-136.

35. Gong, L.-X.; Pei, Y.-B.; Han, Q.-Y.; Zhao, L.; Wu, L.-B.; Jiang, J.-X.; Tang, L.-C., Polymer Grafted Reduced Graphene Oxide Sheets for Improving Stress Transfer in Polymer Composites. *Compos. Sci. Technol.* **2016**, *134*, 144-152.

36. Wan, Y.-J.; Yang, W.-H.; Yu, S.-H.; Sun, R.; Wong, C.-P.; Liao, W.-H., Covalent Polymer Functionalization of Graphene for Improved Dielectric Properties and Thermal Stability of Epoxy Composites. *Compos. Sci. Technol.* **2016**, *122*, 27-35.

37. Hu, Z.; Huang, Y.; Wang, F.; Yao, Y.; Sun, S.; Li, Y.; Jiang, Z.; Xu, H.; Tang, P., Synthesis of Novel Single-Walled Carbon Nanotubes/Poly (P-Phenylene Benzobisoxazole) Nanocomposite. *Polym. Bull.* **2011**, *67*, 1731-1739.

38. Zhou, C.; Wang, S.; Zhang, Y.; Zhuang, Q.; Han, Z., In Situ Preparation and Continuous Fiber Spinning of Poly(P-Phenylene Benzobisoxazole) Composites with Oligo-Hydroxyamide-Functionalized Multi-Walled Carbon Nanotubes. *Polymer* **2008**, *49*, 2520-2530.

Could you insert these references at the appropriate point??

[9] Wang, H.; Griffiths, J.-P.; Egdell, R. G.; Moloney, M. G.; Foord, J. S. Chemical Functionalization of Diamond Surfaces by Reaction with Diaryl Carbenes. *Langmuir* 2008, 24, 862–868.

[11] C.L. Bagwell, D.M.L. Leonard, J.P. Griffiths, M.G. Moloney, N.J. Stratton, D.P. Travers, Post-polymerization modification of materials using diaryldiazomethanes: changes to surface macroscopic properties, *Macromol. React. Eng.* 8 (2014) 170-180.

[12] K. Awenat, P.J. Davis, M.G. Moloney, W. Ebenezer, A chemical method for the convenient surface functionalisation of polymer, *Chem. Commun.* 8 (2005) 990-992.

[16] J.P. Griffiths, D.M.L. Leonard, M.G. Moloney, N. J. Stratton, Control of wetting behavior using post-polymerization modifications of surface chemical functionality, *J. Mol. Eng. Mater.* 1 (2012) 1250002-9.

[17] P. Luksirikul, B. Ballesteros, G. Tobias, M.G. Moloney, M.L.H. Green, pH-triggered release of materials from single-walled carbon nanotubes using dimethylamino-functionalized fullerenes as removable “corks”, *Carbon* 48 (2010) 1912-1917.